

Benchtop and animal validation of a portable fluorescence microscopic imaging system for potential use in cholecystectomy

Jian Ye
Guanghai Liu
Peng Liu
Shiwu Zhang
Pengfei Shao
Zachary J. Smith
Chenhai Liu
Ronald X. Xu

Benchtop and animal validation of a portable fluorescence microscopic imaging system for potential use in cholecystectomy

Jian Ye,^{a,†} Guanghui Liu,^{a,†} Peng Liu,^a Shiwu Zhang,^a Pengfei Shao,^a Zachary J. Smith,^a Chenhai Liu,^b and Ronald X. Xu^{a,c,*}

^aUniversity of Science and Technology of China, Department of Precision Machinery and Precision Instrumentation, Hefei, Anhui, China

^bAnhui Provincial Hospital, Department of General Surgery, Hefei, Anhui, China

^cOhio State University, Department of Biomedical Engineering, Columbus, Ohio, United States

Abstract. We propose a portable fluorescence microscopic imaging system (PFMS) for intraoperative display of biliary structure and prevention of iatrogenic injuries during cholecystectomy. The system consists of a light source module, a camera module, and a Raspberry Pi computer with an LCD. Indocyanine green (ICG) is used as a fluorescent contrast agent for experimental validation of the system. Fluorescence intensities of the ICG aqueous solution at different concentration levels are acquired by our PFMS and compared with those of a commercial Xenogen IVIS system. We study the fluorescence detection depth by superposing different thicknesses of chicken breast on an ICG-loaded agar phantom. We verify the technical feasibility for identifying potential iatrogenic injury in cholecystectomy using a rat model *in vivo*. The proposed PFMS system is portable, inexpensive, and suitable for deployment in resource-limited settings. © 2018 Society of Photo-Optical Instrumentation Engineers (SPIE) [DOI: 10.1117/1.JBO.23.2.020504]

Keywords: fluorescence microscopic imaging; cholecystectomy; image-guided surgery; biliary injuries.

Paper 170600LRR received Oct. 10, 2017; accepted for publication Jan. 19, 2018; published online Feb. 22, 2018.

Cholecystectomy is a commonly used clinical procedure for the treatment of many biliary tract diseases, such as acute cholecystitis, gallstones, biliary obstruction, and biliary colic. However, this procedure is associated with a complication rate of 0.45%.¹ Once complications occur after cholecystectomy, the patient suffers from continuously repeated treatments, with potentially seriously life-threatening results.² Previously, Asbun et al.³ found that the main cause for cholecystectomy-associated complications was the misidentification of the biliary system due to

inflammation, adhesion, fat, and the patients' other clinical conditions. Clinically, intraoperative cholangiography is applied to prevent iatrogenic biliary injuries.⁴ But the operation procedure is complicated and involves a certain risk of wound infection.⁵ The intracorporeal ultrasound and magnetic resonance cholangio-pancreatography represent that other modalities are commonly used for diagnosis and preoperative detection of biliary injuries.⁶ These methods are resource, labor, and time intensive, require a high level of technical skills for clinicians, and are not suitable for real-time cholangiography.

In recent years, there has been an increasing interest in using near-infrared fluorescence imaging technology for surgical navigation.⁷ It has been used for sentinel lymph node mapping to treat breast cancer, liver cancer resection, and biliary system imaging.^{8,9} Indocyanine green (ICG) is a safe and effective near-infrared fluorescent dye already approved by the FDA for use in humans. It can effectively penetrate skin, gallbladder, bile duct, and other tissues to a depth of 5 to 8 mm.¹⁰

In this letter, we report a low-cost and portable fluorescence microscopic system (PFMS) that uses near-infrared fluorescence imaging to guide cholecystectomy. The PFMS device comprises a light source module, a detection module, and a Raspberry Pi computer, as shown in Figs. 1(a) and 1(b). The light source module consists of eight 690-nm LEDs for excitation and one 850-nm LED for background illumination, as shown in Fig. 1(c). The power distribution of the excitation light is simulated by the TracePro software package. The averaged intensity of the excitation light source is 143 W/m², and the maximal intensity is 180 W/m². The surgical field is 40 mm × 40 mm, and the working distance is 50 mm. With numerical simulation, we are able to optimize the arrangement of the LED locations for uniform light distribution without irreversible photobleaching [Fig. 1(d)]. Based on Fig. 1(e), the light distribution measured by experiment coincides with that of simulation.

The detection module consists of a 5-megapixel OV5647 CMOS camera (OmniVision, Santa Clara, California) coupled with a ML15 lens system (Meimei Metering Electricity Technology Co., Shanghai, China) and a BLP01-785R optical filter (Semrock Inc., New York). The filter is placed between the lens system and the camera, with its angle of incidence and cut-off wavelength carefully designed to ensure appropriate fluorescence detection in the desired field of view. The detection module has an adjustable magnification from 0.13× to 2×. A Raspberry Pi computer is used for the primary imaging acquisition and analysis tasks, including synchronization of fluorescence excitation and background illumination, acquisition of fluorescence and background image, and image fusion at a frame rate of two frames per second.

Fluorescence imaging performance of our PFMS system is characterized at different ICG concentrations and compared with that of an *in vivo* Imaging System (IVIS) Lumina III small animal imaging system (PerkinElmer, Waltham, Massachusetts). According to Fig. 2(a), our PFMS system has a sensitivity similar to that of the IVIS system in an ICG concentration range from 0 to 0.1 mg/mL, with the peak fluorescence emission achieved at 0.008 mg/mL, which is fully consistent with the former research by Yuan et al.¹¹ We have also evaluated the imaging depth of the system by embedding an agar phantom of ICG at 0.008 mg/mL in chicken breast tissue of different thicknesses. According to Figs. 2(b) and 2(c), while the turbid nature of the tissue precludes imaging at depths much >2 mm, the signal still remains marginally above

*Address all correspondence to: Ronald X. Xu, E-mail: xu.ronald@hotmail.com

†These authors contributed equally to this work.

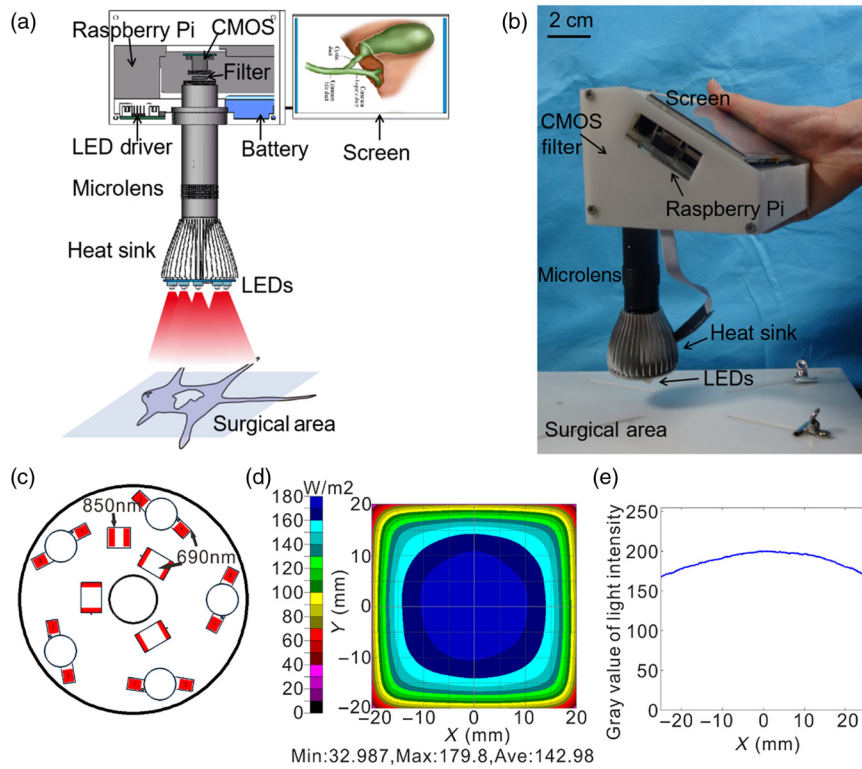


Fig. 1 Design of the PFMS device and the light source module: (a) schematic of the PFMS system, (b) photographic image of the PFMS prototype, (c) LED layout on an aluminum substrate, (d) simulated distribution of light intensity at a working distance of 50 mm, and (e) the actual distribution of excitation light intensity at the LED working distance of 50 mm.

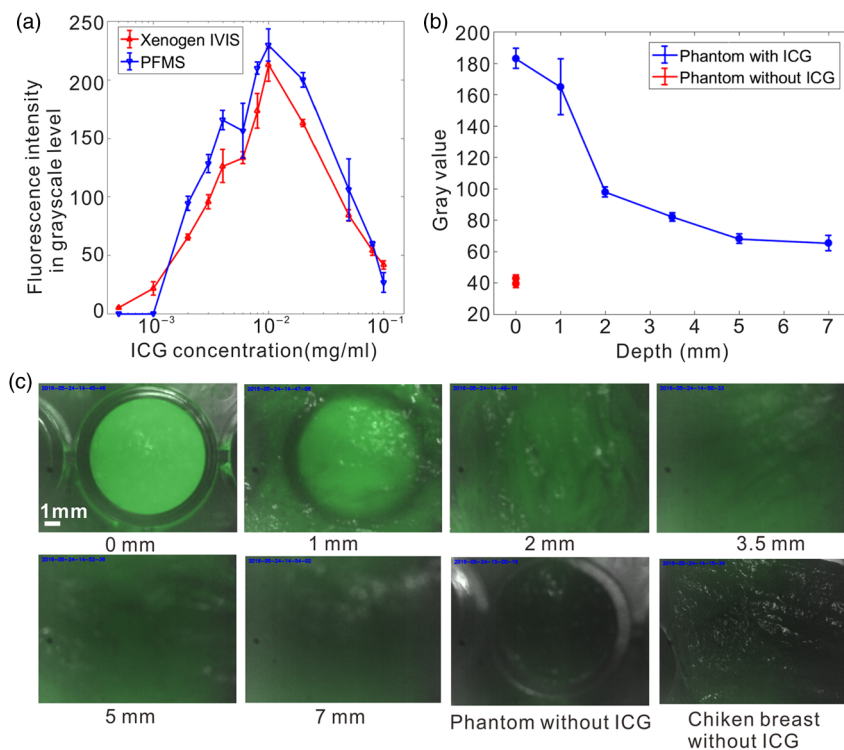


Fig. 2 Fluorescence imaging characterization of the PFMS system: (a) comparison of fluorescence intensities measured by the PFMS system and the Xenogen IVIS system at different ICG concentration levels, (b) gray value of the fluorescence image at different tissue depths, and (c) fluorescence images acquired by the PFMS system through chicken breast tissue of different thicknesses.

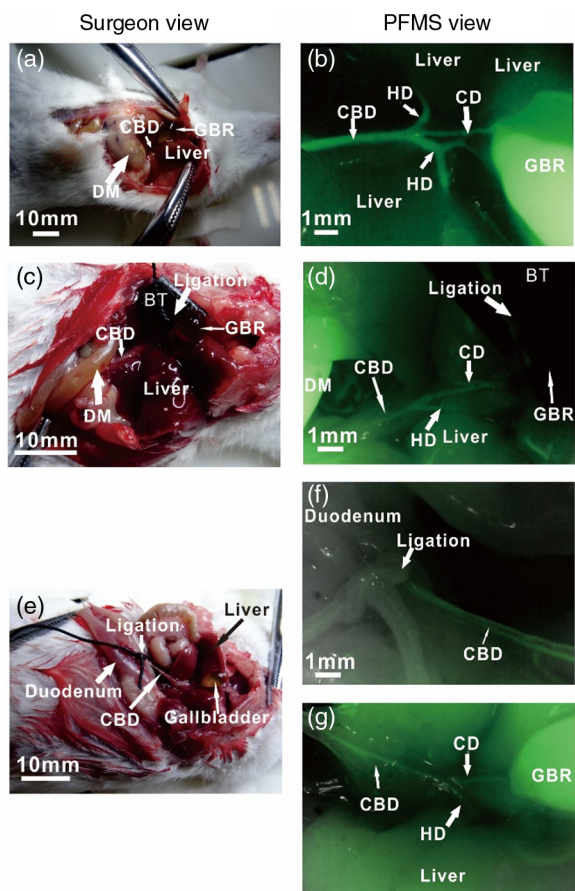


Fig. 3 Photographic and fluorescence images of the rats after different cholecystectomy procedures: (a, b) NL, (c, d) CL, (e, f, g) CBL. (f) and (g) are fluorescence images acquired near duodenum and common bile duct, respectively. CBD, common bile duct; HD, hepatic bile duct; CD, cystic duct; DM, duodenum; and GBR, gall bladder.

background out to 5 to 7 mm, suggesting that fluorescence signals from buried objects may be sensed (albeit with low SNR) at this depth.

Furthermore, *in vivo* validation of the PFMS system is carried out following the animal protocol approved by the Animal Care and Use Committee at the School of Life Sciences of University of Science and Technology of China (Protocol No. USTCACUC1501015). A total of nine adult female rats (Beijing Vital River Laboratory Animal Technology Co. Ltd., Beijing, China) with a weight of 25 to 35 g are equally divided for the following procedures: (1) no ligation (NL), (2) cystic duct ligation (CL, simulating correct cholecystectomy), and (3) common bile duct ligation (CBL, simulating incorrect cholecystectomy). Each animal is anaesthetized and fixed by medical tape, with its hepatobiliary system exposed by laparotomy. The PFMS device is used to guide the NL, CL, and CBL procedures, respectively, followed by tail vein injection of 0.2 mL ICG solution at a concentration of 0.01 mg/mL for fluorescence imaging at an interval of 5 min for 2.5 h. Figure 3 shows the representative background (left column) and fluorescence (right column) images acquired by the PFMS device after each procedure. According to Figs. 3(a) and 3(b), strong fluorescence emission is observed in the biliary structure and the gall bladder, indicating NL. According to Figs. 3(c) and 3(d), the gall

bladder shows markedly reduced fluorescence emission, indicating appropriate ligation of cystic duct. According to Figs. 3(e) to 3(g), fluorescence emission is observed in the gall bladder but absent from the duodenum, indicating iatrogenic ligation of common bile duct.

In summary, we propose a PFMS device for simultaneous background and fluorescence imaging of biliary structure during cholecystectomy. In comparison with other cholangiographic techniques, the proposed device has advantages of simple operation, portability, and real-time imaging at low cost without radiation hazard. Our benchtop study demonstrates that the PFMS device has imaging sensitivity and dynamic range similar to that of a commercial Xenogen IVIS system. Our *in vivo* study demonstrates the technical feasibility for precise localization of the biliary structure and identification of potential iatrogenic injury. Considering that human biliary size and anatomy are different from that of a rat, this letter only demonstrates the technical feasibility of biliary imaging without further assessment of the clinical feasibility of reduced postoperative complications. Further validation tests in large animals are necessary before clinical deployment of such a device. In addition to cholecystectomy, this device may find use in many other surgical procedures where fluorescence imaging is needed at both microscopic and macroscopic levels.

Disclosures

The authors have no relevant financial interests in this letter and no potential conflicts of interest relevant to disclose.

Acknowledgments

The project was partially supported by the National Natural Science Foundation of China (Nos. 81271527 and 81327803) and the Fundamental Research Funds for the Central Universities (No. WK2090090013). The authors are grateful for the help from Dr. Ting Yue, University of Science and Technology of China (USTC), School of Life Sciences and Zelin Yu (USTC, Department of Precision Machinery) in performing the ICG concentration experiment, Meng Li and Shulin Zhang (USTC, Department of Precision Machinery) for assistance with programming, Rong Ma (Chongqing Medical University) for assistance with animal experiments, and Chaoyu Yang (USTC, Department of Precision Machinery) for assistance with 3-D printing.

References

1. J. P. Dolan et al., "Ten-year trend in the national volume of bile duct injuries requiring operative repair," *Surg. Endosc.* **19**(7), 967–973 (2005).
2. S. Connor and O. J. Garden, "Bile duct injury in the era of laparoscopic cholecystectomy," *Br. J. Surg.* **93**(2), 158–168 (2006).
3. H. J. Asbun et al., "Bile duct injury during laparoscopic cholecystectomy: mechanism of injury, prevention, and management," *World J. Surg.* **17**(4), 547–551 (1993).
4. N. N. Massarweh and D. R. Flum, "Role of intraoperative cholangiography in avoiding bile duct injury," *J. Am. Coll. Surg.* **204**(4), 656–664 (2007).
5. E. Tanaka et al., "Real-time intraoperative assessment of the extrahepatic bile ducts in rats and pigs using invisible near-infrared fluorescent light," *Surgery* **144**(1), 39–48 (2008).
6. S. J. Dalton, S. Balupuri, and J. Guest, "Routine magnetic resonance cholangiopancreatography and intra-operative cholangiogram in the evaluation of common bile duct stones," *Ann. R. Coll. Surg. Engl.* **87**(6), 469–470 (2005).

7. Q. T. Nguyen and R. Y. Tsien, "Fluorescence-guided surgery with live molecular navigation—a new cutting edge," *Nat. Rev. Cancer* **13**(9), 653–662 (2013).
8. S. L. Troyan et al., "The FLARE™ intraoperative near-infrared fluorescence imaging system: a first-in-human clinical trial in breast cancer sentinel lymph node mapping," *Ann. Surg. Oncol.* **16**(10), 2943–2952 (2009).
9. Y. Kono et al., "Techniques of fluorescence cholangiography during laparoscopic cholecystectomy for better delineation of the bile duct anatomy," *Medicine* **94**(25), e1005 (2015).
10. T. Desmettre, J. Devoisselle, and S. Mordon, "Fluorescence properties and metabolic features of indocyanine green (ICG) as related to angiography," *Surv. Ophthalmol.* **45**(1), 15–27 (2000).
11. B. Yuan, N. Chen, and Q. Zhu, "Emission and absorption properties of indocyanine green in Intralipid solution," *J. Biomed. Opt.* **9**(3), 497–503 (2004).